Naval Research Laboratory

Washington, DC 20375-5320

NRL/MR/6720--06-8956

Alternate Approaches to Laser Guided Discharges

J. DAVIS
R.E. TERRY
G.M. PETROV
A.L. VELIKOVICH

Radiation Hydrodynamics Branch
Plasma Physics Division

April 19, 2006

REPORT DOCUMENTATION PAGE

Form Approved
OMB No. 0704-0188

1. REPORT DATE *(DD-MM-YYYY)*	**2. REPORT TYPE**	**3. DATES COVERED** *(From - To)*
19-04-2006	Memorandum Report	

4. TITLE AND SUBTITLE

Alternate Approaches to Laser Guided Discharges

5a. CONTRACT NUMBER

5b. GRANT NUMBER

5c. PROGRAM ELEMENT NUMBER

6. AUTHOR(S)

J. Davis, R.E. Terry, G.M. Petrov, and A.L. Velikovich

5d. PROJECT NUMBER

5e. TASK NUMBER

5f. WORK UNIT NUMBER
67-3825-06

7. PERFORMING ORGANIZATION NAME(S) AND ADDRESS(ES)

Naval Research Laboratory, Code 6720
4555 Overlook Avenue, SW
Washington, DC 20375-5320

8. PERFORMING ORGANIZATION REPORT NUMBER

NRL/MR/6720--06-8956

9. SPONSORING / MONITORING AGENCY NAME(S) AND ADDRESS(ES)

Office of Naval Research
One Liberty Center
875 North Randolph St.
Arlington, VA 22203-1995

10. SPONSOR / MONITOR'S ACRONYM(S)

11. SPONSOR / MONITOR'S REPORT NUMBER(S)

12. DISTRIBUTION / AVAILABILITY STATEMENT

Approved for public release; distribution is unlimited.

13. SUPPLEMENTARY NOTES

This research was funded in connection with 6.1 Physics of Strong Laser Fields and Laser Induced Coulomb Explosion

14. ABSTRACT

We propose a novel use of laser induced breakdown channels to establish a transmission line through air, which terminates at a distant load object.

15. SUBJECT TERMS

Laser guided discharge
Air chemistry
Propagation

16. SECURITY CLASSIFICATION OF:			**17. LIMITATION OF ABSTRACT**	**18. NUMBER OF PAGES**	**19a. NAME OF RESPONSIBLE PERSON**
					Robert E. Terry
a. REPORT	**b. ABSTRACT**	**c. THIS PAGE**	UL	25	**19b. TELEPHONE NUMBER** *(include area code)*
Unclassified	Unclassified	Unclassified			(202) 767-6782

CONTENTS

Alternate Approaches to Laser Guided Discharges

J. Davis, R. E. Terry, G. Petrov, A. Velikovich
Plasma Physics Division, Naval Research Laboratory
Washington, D. C. 20375

1 Introduction

The propagation of intense ultrashort laser pulses in the atmosphere is currently under intensive investigation because of its potential for a number of applications, particularly for the generation of super continuum or white light radiation, LIDAR, sensor and detector areas and as a trigger for streamers in air for initiating lightning [26],[23],[33],[10],[19]. In addition, it has the potential for directed energy and possibly for IED neutralization applications. A desired property of ultrashort laser pulses injected into the air is their potential to propagate large distances, producing fairly uniform ionized channels on their wake. This feature of producing long narrow plasma channels is an important property for weapons applications. However, although the laser is excellent for causing air breakdown and creating the plasma channel, very little energy is transported to prospective targets to induce significant damage. A way to improve this deficiency is to launch an electrical discharge [32],[14],[18],[40],[37] through the plasma channel. Laser guided discharges are under intensive investigation for triggering lightning in order to divert the lightning from striking power stations. These applications have been discussed in a number of papers. Our interest in laser guided discharges is the potential to control and to stabilize the directionality of the discharge path, while maintaining the channel and projecting enough energy to cause damage to a test object. The concept that we propose is based on a complete circuit, equivalent to a transmission line, between a laser source and a distant object. In order to explore further this aspect of laser discharge plasma channels it is necessary to determine both the nature of the interaction of the laser with the atmosphere and the ability to deliver interesting amounts of energy to the object.

The interaction of the laser with the ambient air is much more complicated than originally supposed[11],[35],[15],[27],[38],[39]. As the laser interacts with and penetrates the atmosphere it can filament into a number of streamers reducing the power delivered to a distant object. We propose to model and numerically simulate the atmospheric interaction and response of the atmosphere to the propagation of an intense ultrashort IR laser pulse. The atmospheric response to the pulse will be modeled self-consistently coupled to the equations representing the chemistry of reaction kinetics of the atmospheric constituents as the quiescent air is ionized and follow its subsequent return to ambient conditions. It is crucial to determine the lifetime and the length of plasma channels as they develop and evolve if a pulsed IR laser produced plasma channel is to persist long enough to launch an electrical discharge through the plasma channel. The modeling involves numerically solving the propagation equations including a number of important processes such as the nonlinear Kerr effect, self-focusing, Raman scattering, multiphoton / tunneling ionization, air ionization (as an energy loss) and,

Manuscript approved January 20, 2006.

in the case of laser triggered discharges, air chemistry. The equations of propagation have been solved for a number of initial conditions and are well documented in the literature. However, for much of this research a variety of approximations are introduced to avoid the complicated interaction between the laser deposition, hydrodynamic response[21], and the complex of reactions occurring in the air. Real air contains aerosols and water vapor[1] that can severely affect propagation lengths. They can act as nucleation points for ionization and create strong plasma inhomogeneities. Aerosols, dust and other warfighter environments therefore pose additional problems causing laser energy absorption and scattering and allowing air breakdown to occur at even lower laser intensities.

The concept advanced here offers a coordinated path to the practical exploitation of laser guided discharges as energy delivery systems. We discuss the simplest designs for systems of this type as well as the modeling efforts and experimental programs required to reduce them to practice.

2 Background

In order to better understand the first, high voltage phase of the concept and its relation to lightning, the mechanism of a lightning flash is briefly summarized [30],[12].

Clouds can store a tremendous amount of electrostatic energy, which, under the right circumstances, can be released in a lightning flash. The lightning flash is initiated by an electrical breakdown process in the cloud, called preliminary breakdown. This process leads to the creation of a column of charge called stepped leader that travels from cloud to ground (Fig. 1). On its way to the ground the leader may give rise to several branches.

As the stepped leader approaches the ground the electric field at ground level increases. When the stepped leader gets close (a few hundred meters) the electric field at the grounded structure increases to such a level that electrical discharge is initiated from them. This discharge, called connecting leader, travel toward the down-coming stepped leader (Fig. 2). The connecting leader may successfully bridge the gap between the ground and the down-coming stepped leader (Fig.3). The object that initiated the connecting leader is struck by lightning.

Once the connection is made between the stepped leader and ground, a wave of near ground potential travels along the channel toward the cloud. This electromagnetic wave travels at a velocity of nearly the speed of light. This is called the return stroke (Fig.4) and it causes the actual damage. The diameter of the lightning return stroke is typically several centimeters.

The available data indicates that the peak current is 10-100 kA and the energy delivered to the stricken object vary from several MJ to about 1 GJ.

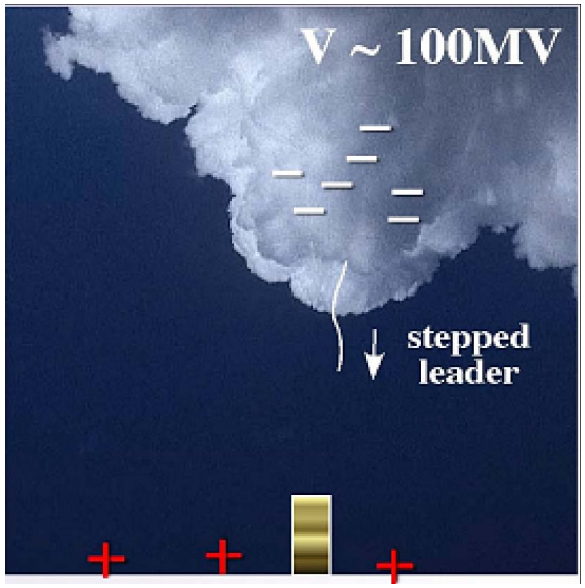

Figure 1: **Downward moving step leader travels from cloud to ground**

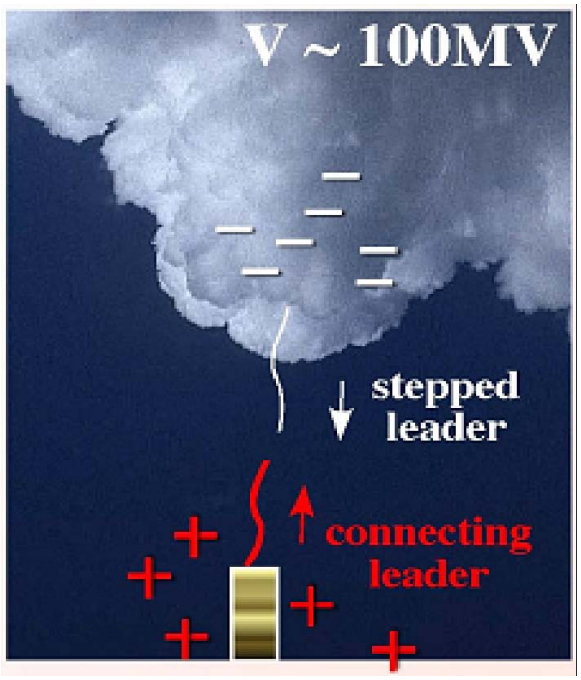

Figure 2: **A connecting leader moving upward is launched from a tall object.**

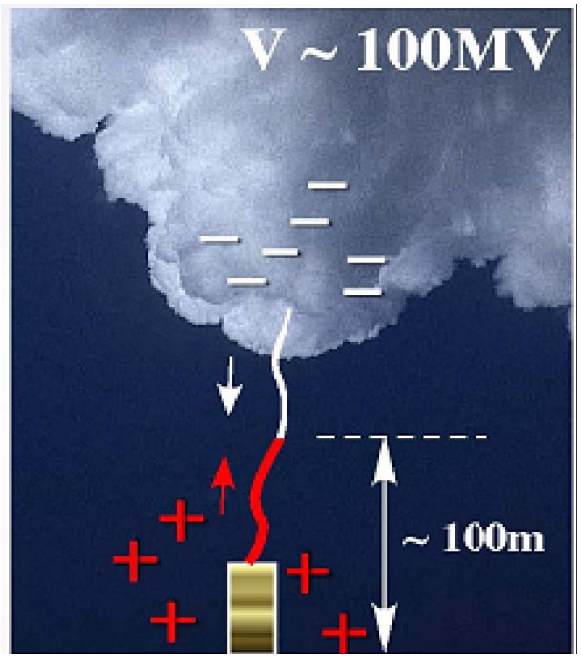

Figure 3: **The connecting leader meets the stepped leader from the cloud.**

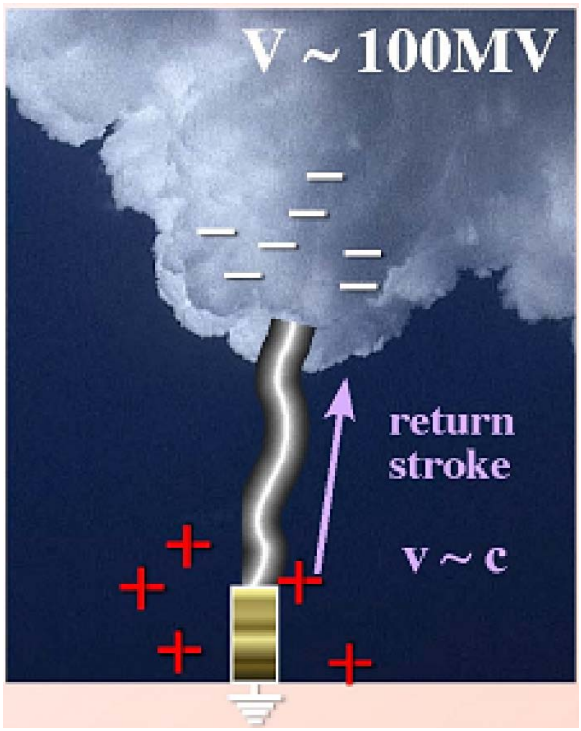

Figure 4: **The return stroke.**

Since the 1970s, many researchers have studied the triggering and guiding of electrical discharges in laboratory with different types of laser systems. The first investigations of laser control of large-scale discharges have been done primarily with long pulse IR lasers. Nevertheless, the use of such lasers suffers from important limitations, leading researchers to consider other candidates, such as long-pulse ultraviolet lasers or, more recently, ultrashort pulse lasers. The advantage of ultrashort laser pulses is their very high intensity, which allows the creation of long continuous plasma channels in air via multiphoton ionization with a modest amount of energy. The plasma channel is used to propagate and guide a plasma wave (leader). The latter is a highly conductive media, which travels from one electrode toward the other. Once the leader bridges the gap between the electrodes, a wave of potential travels along the channel with a speed close to the speed of light delivering MJ levels of energy.

3 Theoretical Description and Operation

The damaging behavior of natural lightning can be enhanced by adding a final pulse power element: closing a circuit and delivering a tailored pulse, similar to the action of a "TASER" device. The reason for having a four-step process (laser created channel-leader-return stroke-final pulse) instead of just one is by far dominated by one factor, viz. the conductivity of the media. Only a medium with very high conductivity is good for delivering a lethal amount of energy to the target. The plasma filaments created by the laser (step one) have low conductivity. During step two (leader propagation) the conductivity of the channel increases by several orders of magnitude. During step three (the return stroke), the channel conductivity increases even further, allowing swift and efficient delivery of energy to the target. During step four (pulse delivery) the ohmic dissipation along the line drives the conductivity up even further. The individual steps will be outlined next.

3.1 Channel Formation

The first part of the problem is to create a plasma channel $\approx 10^2$-10^3 m long. Ultrashort pulse lasers (USPL) are the best candidates for the creation of long continuous plasma channels in air [7],[6],[5],[25],[13],[36],[4],[8],[28],[22],[16],[3]. Nonlinear propagation of ultrashort pulses in air efficiently creates free electrons through multi-photon ionization of oxygen and nitrogen. A plasma channel ($\approx$0.2 mm in diameter) is formed with a typical electron density of n_e $\approx 10^{15}$ –10^{18} cm^{-3} and electron temperature of 1–10 eV. This plasma channel can be very long, hundreds of meters. For example, the generation of long, stable plasma filaments in air over distances in excess of 200 m has been reported[26]. The possibility of creating plasma channels hundreds of meters long is critical for the present application since these filaments can provide a preferred channel for long streamer discharges and guide leaders.

The energy requirements can be estimated as follows. Most of the laser energy is spent for optical field ionization (OFI),

$$\mathcal{E}_{OFI} = n_e V E_{ion} \ , \tag{1}$$

where $V = \pi d^2 L/4$ is the plasma volume and E_{ion} is the ionization energy. For typical values $n_e \approx 10^{16} cm^{-3}$, d = 200 μm, L = 100 – 1000 m , and $E_{ion} \approx 1.2eV = 1.6 \cdot 10^{-18}$ J the laser energy spent for optical field ionization is

$$\mathcal{E}_{OFI} \approx 0.06 - 0.6[J] \ . \tag{2}$$

These energy requirements are not too restrictive, but are certainly still near the upper limit of the presently available USPL systems. What is of primary interest is the time evolution of the channel. After only ≈ 0.1 μs following the plasma channel formation, the electron density (and conductivity) decreases to $n_e \approx 10^{13} cm^{-3}$ and keeps decreasing in time. The electron population doesn't really disappear, but attaches to oxygen, so that an O_2^- ion population arises, which figures heavily in the physics of leader propagation and the subsequent return stroke – a generic population history of these species is shown in Figure 5. According to some analyses, the plasma channel retains properties which are still adequate for triggering and guiding of the discharge for tens of μs, but ultimately, the channel will lose its guiding ability.

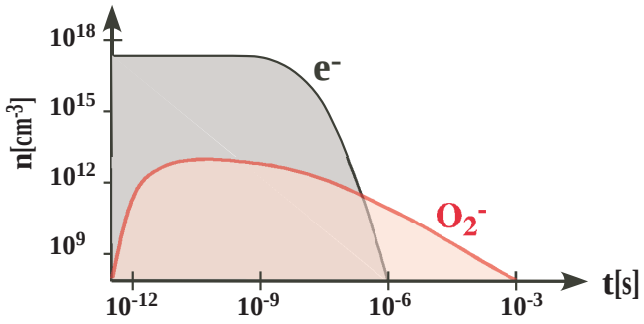

Figure 5: **Conductors in the Laser Induced Breakdown channel.**

3.1.1 Propagation

The model for long-distance propagation is a 2D version of the nonlinear Schrodinger equation for the envelope of the electric field. Our starting point is the wave equation for the

electric field $\mathbf{E}$

$$\left(\nabla_\perp^2 + \frac{\partial^2}{\partial z^2} - \frac{1}{c^2}\frac{\partial^2}{\partial t^2}\right)\mathbf{E} = \mathbf{S} \ , \tag{3}$$

where $\nabla_\perp^2$ is the transverse Laplacian, c is the speed of light, z is the direction of propagation and $\mathbf{S}$ is a source term. The laser electric field, as well as the source term are written as complex amplitudes multiplied by a rapidly varying phase $\psi = k_0 z - \omega_0 t$:

$$\mathbf{E}(r,z,t) = A(r,z,t)e^{i\psi(z,t)}\mathbf{e_x}/2 + c.c. \tag{4}$$

$$\mathbf{S}(r,z,t) = S(r,z,t)e^{i\psi(z,t)}\mathbf{e_x}/2 + c.c. \tag{5}$$

Here $k_0 = \omega_0/c = 2\pi/\lambda$ is the wave number, ω_0 is the laser frequency, $\mathbf{e_x}$ is the unit vector in the direction of polarization and c.c. denotes complex conjugate.

The source term in the right hand side of Eq. (3) consists of several components, which account for the action of the media through which the laser propagates. For the laser intensity and laser pulse duration of interest, the target media can be described as partially ionized plasma. More specifically, it consists of nitrogen and oxygen molecules (the air constituents), their dissociation products, and the plasma that is generated by the leading edge of the laser. For N_2-O_2 mixture at atmospheric pressure and a typical ionization degree of $10^{-7} - 10^{-3}$ the source terms read:

(i) nonlinear contribution for bound electrons, i.e. the Kerr effect:

$$S_{bound} = -\frac{\omega_0^2 n_0^2 n_2}{4\pi c}|A|^2 A = -2k_0^2 n_2 I A \ , \tag{6}$$

(ii) stimulated Raman scattering:

$$S_{Raman} = -4\pi\frac{\omega_0^2}{c^2}\chi_L Q A = -2k_0^2 n_R I A \ , \tag{7}$$

(iii) plasma source term

$$S_{plasma} = \frac{\omega_p^2}{c^2}\left(1 - i\frac{\nu}{\omega_0}\right)A = k_p^2\left(1 - i\frac{\nu}{\omega_0}\right)A \ , \tag{8}$$

(iv) relativistic effects

$$S_{rel} = -\frac{\omega_p^2}{4c^2}\left(\frac{e|A|}{mc\omega_0}\right)^2 A = -k_p^2\left(\frac{e|A|}{2mc\omega_0}\right)^2 A \ , \tag{9}$$

(v) ionization

$$S_{ion} = -8\pi i k_0 \frac{U^{ion}}{c|A|^2}\frac{\partial n_e}{\partial \tau}A = -ik_0\frac{U^{ion}}{I}\frac{\partial n_e}{\partial \tau}A \ . \tag{10}$$

There are several parameters participating in the source terms: n_0 is the refractive index of air, assumed to be unity, n_2 is the nonlinear refractive index of air, $I = \frac{cA^2}{8\pi}$ is the peak laser intensity, χ_L is the laser susceptibility at frequency ω_0, Q is the response function for

stimulated Raman scattering, n_R is an effective nonlinear refractive index due to Raman scattering, ν is electron-neutral collision frequency, $k_p = \omega_p/c$ is the plasma wave number with plasma frequency $\omega_p = (4\pi e^2 n_e/m)^{1/2}$, e and m are the electron charge and mass respectively, n_e is the electron density, $e|A|/(mc\omega_0)$ is the normalized electric field strength, U^{ion} is the ionization potential of O_2, and $\partial n_e/\partial\tau$ is the OFI rate.

An equation suitable for numerical solution is obtained after a sequence of intermediate steps. First, the electric field (4) and source term (5) are inserted into the wave equation (3) and the rapidly varying exponential factor is canceled from both sides of the equation. The resulting equation is further transformed into the so called laser frame by substituting the variables (z,t) with variables (z,τ), where $\tau = t - z/c$ is the retarded time. Finally, the equation is written in the form

$$\nabla_\perp^2 A + 2ik_0\frac{\partial A}{\partial z} - 2\frac{\partial^2 A}{\partial z \partial(c\tau)} + \frac{\partial^2 A}{\partial z^2} - c^2 k_0 \beta_2 \frac{\partial^2 A}{\partial(c\tau)^2} + MA = 0 \ , \tag{11}$$

where

$$M = k_0^2(n_2 + n_R)I - k_p^2\left(1 - i\frac{\nu}{\omega_0}\right) + k_p^2\left(\frac{e|A|}{2mc\omega_0}\right)^2 + ik_0\frac{U^{ion}}{I}\frac{\partial n_e}{\partial\tau}$$

combines the non-derivative terms of the equation, and the transverse Laplacian in cylindrical geometry reads $\nabla_\perp^2 A = \frac{1}{r}\frac{\partial}{\partial r}\left(r\frac{\partial A}{\partial r}\right)$. The term $c^2 k_0 \beta_2 \frac{\partial^2 A}{\partial(c\tau)^2}$ is the so-called Group Velocity Dispersion (GVD), which accounts for the frequency dependence of the refractive index of air. In the transformed coordinates time τ refers to the front of the laser pulse. Therefore A is always bounded between 0 and R in radial direction and 0 and T in the time domain, where R is an appropriate distance from the axis, much larger compared to the laser pulsewidth, and T is the laser pulse duration. Equation (11) is a partial differential equation, which is solved using finite differences by advancing the laser electric field amplitude $A(r,\tau)$ forward, in $+z$ direction.

Initial and boundary conditions are required to solve Eq. (11). The initial condition at $z = 0$ comes from the imposed laser intensity profile $I_0(r,\tau)$ upon entering the computational domain. The input laser field is then

$$A(r, z = 0, \tau) = (8\pi I_0(r,\tau)/c)^{1/2} \ , \tag{12}$$

while the boundary conditions read:

$$\begin{aligned} \partial A(r = 0, z, \tau)/\partial r = 0 \ , \\ A(r = R, z, \tau) = 0 \ , \\ A(r, z, \tau = 0) = 0 \ , \\ A(r, z, \tau = T) = 0 \ . \end{aligned}$$

The laser propagation in air creates plasma through OFI. The plasma filaments have local electron density determined by the electron continuity equation

$$\frac{\partial n_e}{\partial\tau} = W_{OFI} n_{O_2} \ . \tag{13}$$

with boundary condition $n_e(r, z, \tau = 0) = 0$. In (13) the terms W_{OFI} and n_{O_2} are the OFI rate, which is a strong function of the laser intensity and the density of oxygen molecules, respectively. The plasma generation is included into the propagation equation via three terms, (8,9,10). The real part of (8) and the term (9) are "conservative", i.e. they only focus or difract the laser beam without causing any loss of energy. The imaginary part of (8), as well as the last term, (10), are depleting the laser beam energy by heating the electrons through Inverse Bremsstrahlung (IB) and ionization, respectively. The energy balance equation, derived from Eq. (11), reads:

$$\frac{dE}{dz} = \int_0^r \int_0^T 2\pi r[\frac{\partial n_e}{\partial \tau} U^{ion} - \frac{\omega_p^2(r)\nu}{\omega_0^2 c} I(r)]drd\tau. \tag{14}$$

Equation (14) states that as the laser advances it loses energy in ionization (the first integrand term on the right hand side of (14)) and IB (the second integrand term). Equations (11)-(13) form a complete system of equations for the laser electric field, laser intensity and electron density.

3.2 Leader Propagation

Leader propagation guided by a high intensity USPL has been conclusively demonstrated by several research groups. For example, one of them has performed an extensive study of laser-induced discharges in the classical configuration of rod-plane gaps of several meters, in appropriate conditions, and obtained free, stable propagation of positive leaders. These experiments showed that a plasma channel created with an USPL can trigger leader propagation at a reduced voltage and guide it on a distance of a few meters [20],[34],[29],[2].

The leader is a thin (≈mm) highly conductive filament that starts from the active electrode and propagates toward the grounded electrode (or earth). The strong electric field in front of the leader ionizes the gas and creates streamers, which the leader engulfs and advances. In general, leaders can be incepted and propagate in air without a plasma channel (lightning is a typical example). In this situation the leader path, however, is to some degree random and the leader can go virtually anywhere. Therefore, in order to successfully bridge (and short-circuit) the gap between high-voltage source and an object, the leader must be "guided". Hence the plasma channel formation is an integral part of the process. There are additional benefits of the plasma channel. The presence of the channel alleviates the conditions for leader inception (lower breakdown voltage) and increases the leader velocity by a factor of ten compared to natural leader. The first benefit directly affects the requirements and design of the power supply. The second one may be a lot more important for long-distance guiding of leaders as the leader channel may be capable of guiding for only a limited period of time (10 – 100 μs) and higher leader velocity means longer guiding distance.

Since the whole process of delivering a lethal amount of energy to the target is driven by the channel conductivity, it is instructive to compare the plasma conductivity of the laser

created channel (step one) and the leader (step two). Such a comparison would explain the necessity of this stage. During step two (leader propagation) the channel resistance decreases by several orders of magnitude, as it can be seen from the following table.

Table 1: Channel Parameters Compared

Parameter	plasma channel	leader	return
Length [m]	100-1000	100-1000	100 - 1000
Diameter [cm]	0.02	0.2	2.0
Gas temperature [K]	300	3000	20000
Neutral density [cm^{-3}]	$2.5x10^{19}$	$2.5x10^{18}$	$5.0x10^{17}$
Electron density [cm^{-3}]	10^{13}	10^{13}	$5.0x10^{17}$
Conductivity [Ω^{-1} cm^{-1}]	10^{-3}	10^{-2}	10^{-1}
Resistance [Ω cm^{-1}]	$3x10^{6}$	$3x10^{3}$	$3.0x10^{-3}$
Current [A]	$3x10^{-3}$	3	3000

As can be seen from the table, during the second step the channel resistance per unit length decreases by a factor of thousand, both due to increased conductivity and increased channel cross section $S = \pi d^2/4$. The current flowing through the channel increases accordingly, which causes further gas heating and channel expansion. At the end, the conductivity suitable for the "return stroke" is realized.

3.3 Pulse Power

The energy delivery technology of interest comprises two subsystems: a high voltage leader propagation interface and a low voltage transmission line for final pulse delivery.

3.3.1 High Voltage

The schematic representation of the transmission line interface to the systems described above is shown in Figure 6. The plane parallel capacitor faces are shown perforated by a laser beam convolute. A high breakdown strength dielectric occupies the space immediately adjacent to the convolute and is shown there with a gas gap at NTP between it and the laser beam convolute.

In the early high voltage phase of operation the initial laser channels are quite resistive (1.2 – 3.0 kΩ/cm) and support only minimal currents. Connected to the hot side of their respective capacitors through a convolute, an assessment must be made of the leakage currents to the ground plane of the capacitor through the gas gap around the laser beam convolute. If these

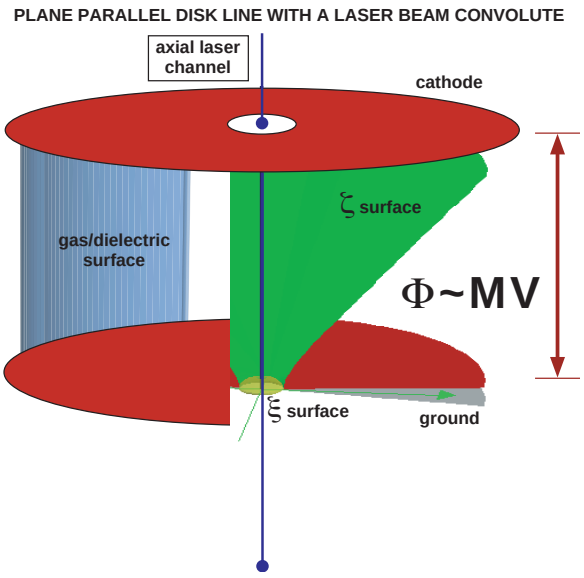

Figure 6: **Transmission Line Interface**

currents are too great, leader propagation will not be supported and a hard electrical contact to the load will fail.

Making the approximation that the laser beams don't heavily perturb the capacitor fields where the convolutes are, the expected leakage currents can be estimated from those fields and an estimate of gap conductivity alone. As shown in Figure 7, which uses the analytic unperturbed electrostatic potential solution (in planar oblate spheroidal coordinates),

$$\Phi(\xi,\zeta) = E_0 a \xi [\zeta - \frac{(\zeta cot^{-1}(\zeta) - 1)}{\pi}] \tag{15}$$

with a characteristic length (**a**, the hole radius) and E_0 a characteristic field strength for the capacitor, see also [31]. Examining the field components, the field E_ξ is the radial component near the axis. Once the laser beam convolute is made small compared with the hole size, this mostly radial field component will be only about 0.05 E_0. The orthogonal component, mostly axial, aligns with the unperturbed field of the plane parallel disk feed far from the hole.

Using a typical electron density of corona discharge in air at perhaps about 10^{11} cm^{-3}, the expected resistance for the parasitic radial current can be approximated by

$$R_{leak} = f_{geo}(\frac{10^{11}}{n_e})(\frac{6.5}{l_{cap}})[k\Omega] \tag{16}$$

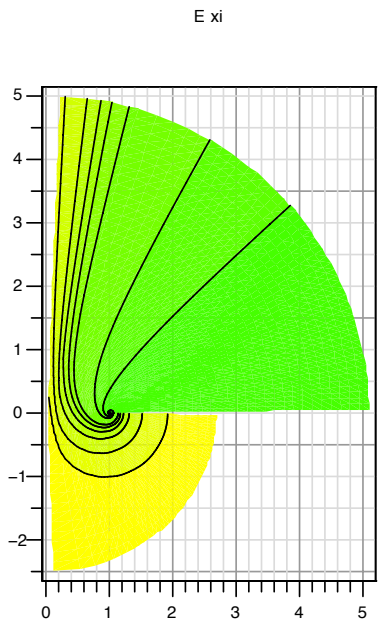

Figure 7: ξ **Field Strength Contours**

with f_{geo} a factor of order one, and l_{gap} the physical size of the capacitor separation. When such an estimate is used in a parallel resistive current division of channel current and parasitic current, the expected leakage current ratio can be written,

$$\frac{I_{leak}}{I_{chan}} \approx (\frac{0.01}{f_{geo}})(L_{gap}l_{cap})(\frac{n_e}{10^{11}}). \tag{17}$$

The field pattern just described around the convolute can only persist for the duration of the high voltage phase. As a return stroke along the laser channels brings the conductivity up by several orders of magnitude, this field pattern will shift to that of a conventional post hole convolute with a larger radial field strength. Balancing that radial electrical stress will depend upon: (i) the time developing drop in the voltage across the disk feed, (ii) the increase of magnetic insulation around the laser channel, and (iii) the dielectric strength of the feed. The end state of that process is a disk feed at ground potential perforated by a highly conductive laser channel.

3.3.2 Laser Channel Transmission Line

Once formed the laser channels and their connected circuit through a load can be considered as a twin lead or Lecher line – described by macroscopic specific capacitance, inductance, and series or shunt resistances as shown in Figure 8.

Owing to the resistance per unit length $\hat{\rho}$ in the laser channels forming this line, with a separation h and a conductor diameter d, it is described by a line impedance

$$Z_{line} = 120 \ln \left(\frac{h}{d} + \sqrt{(\frac{h}{d})^2 - 1} \right) \quad [\Omega], \tag{18}$$

for a finite sized cylindrical conductor pair and the lossy Telegrapher's equation for voltages. With $g\left(x,t\right) = V_{forward} + V_{backward}$,

$$\frac{\partial^2 g\left(x,t\right)}{\partial x^2} + \delta \frac{\partial g\left(x,t\right)}{\partial x} = \frac{\partial^2 g\left(x,t\right)}{c^2 \partial t^2} \ . \tag{19}$$

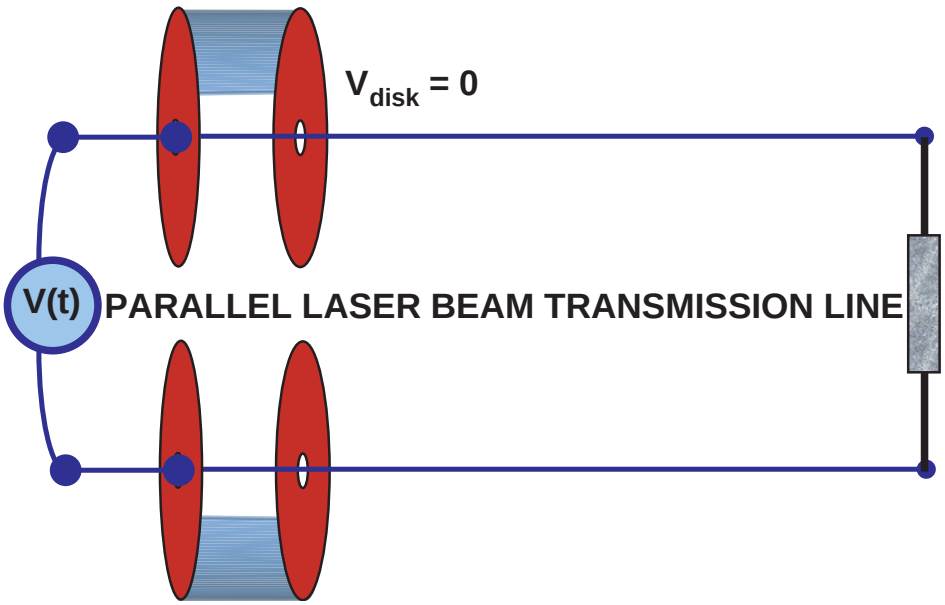

Figure 8: **Final Transmission Line**

The series resistance along the plasma channel conductors is now represented by the spatial damping decrement, δ, which is the channel resistance per unit length $\hat{\rho}$ divided by the line impedance, Z_{line}. Explicit losses due to shunt resistances along the line, were the two channels to establish a conducting path between them, would be described by an additional temporal damping term.

The forward and backward signals (c.f. Figure 9) on a uniform lossy line of this nature can be represented by the following fundamental solutions, parameterized by the free space wavelength λ,

$$V_{forward} = \cos\left(2\,\pi\,\left(\xi - \tau\,\left(1 + 1/16\,\frac{\eta^2}{\pi^2}\right)\right)\right) e^{-1/2\,\eta\,\xi} \tag{20}$$

$$V_{backward} = \frac{(\kappa - 1)}{(\kappa + 1)} \cos\left(2\,\pi\,\left(\xi + \tau\,\left(1 + 1/16\,\frac{\eta^2}{\pi^2}\right)\right)\right) e^{-1/2\,\eta\,(\Xi - \xi)} \tag{21}$$

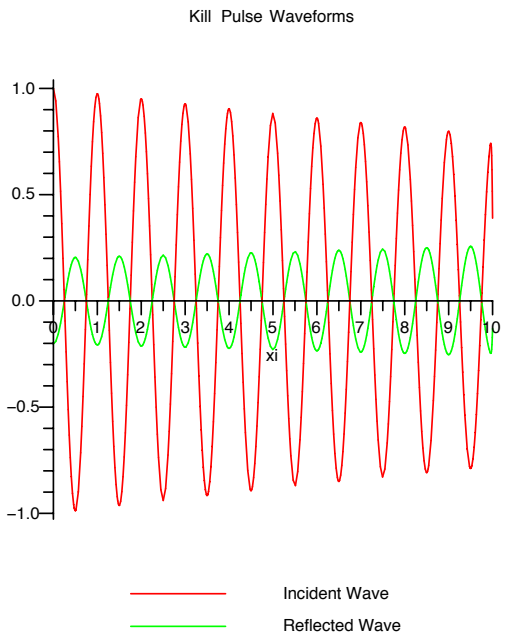

Figure 9: **Transmission Line Waveforms**

where $\xi = x/\lambda$, $\tau = \nu t$, and D_{Load} represents the distance to the load.

As shown in these equations, three fundamental dimensionless parameters $\kappa = \frac{Z_{load}}{Z_{line}}$, $\eta = \frac{\hat{\rho}\lambda}{Z_{line}}$, and $\Xi = \frac{D_{Load}}{\lambda}$ span the solution space. The effective reflection coefficient at the terminating resistive load is just $\frac{(\kappa-1)}{(\kappa+1)}$ and is invariant for impedance ratios which are the inverse of one another. Everything of relevance for power transfer to a load can be specified as a function of $[\Xi, \eta, \kappa]$, e.g. the coupling fraction shown in Figure 10 as function of κ with

[Ξ=10, η=0.05]. The line also admits some dispersion in that,

$$\omega\left(k_0\right) = \omega_0 \sqrt{1 + 1/16 \, \frac{\hat{\rho}^2 {\lambda_0}^2}{{Z_{line}}^2 \pi^2}} \tag{22}$$

as shown in Figure 11. Under most conditions, this dispersion doesn't lower the group velocity significantly.

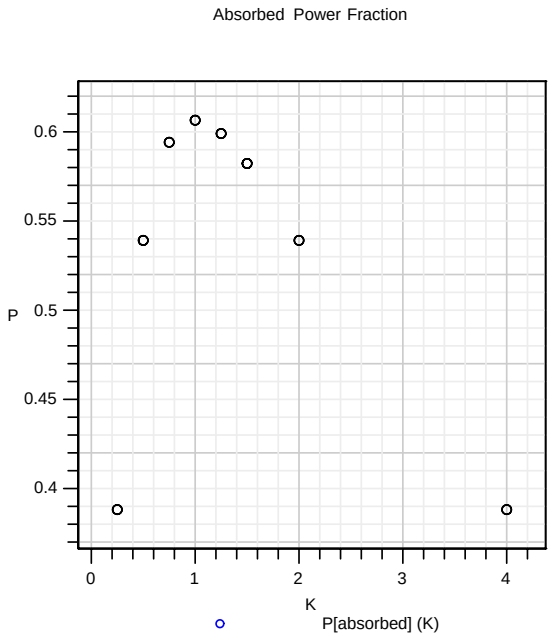

Figure 10: **Transmission Line Coupling**

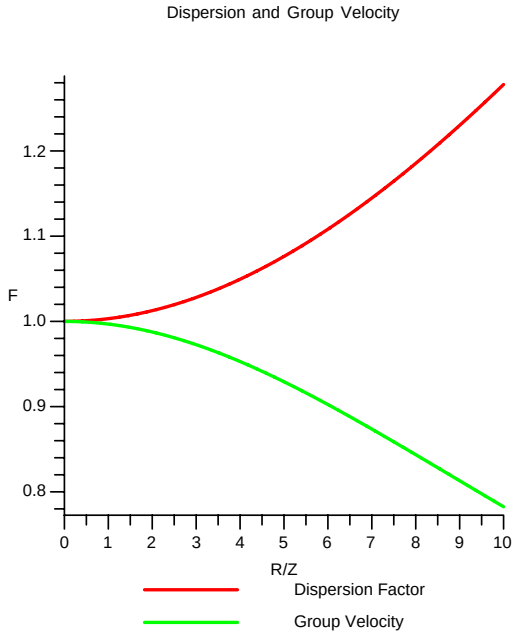

Figure 11: **Dispersion Characteristics**

4 Proof of Principle Experiments

An operational system is thus decomposed into the four distinct phases discussed above. It is certainly possible to test the behaviors of each component in an experiment of modest distance (≈100 m) and, once successful, the development to a system of interest to the services is then only a factor ten.

4.1 Laser Propagation and Channel Formation

There exist currently available laser systems which can be used for the initial experiment. One commonly known variety is the Ti-sapphire system, which might offer the parameters:

- wavelength – 795 nm,
- energy – 10 to 50 mJ,
- pulse duration – 100 to 1000 fs,
- power – 10 to 100 GW,
- and filament lengths of 200 m.

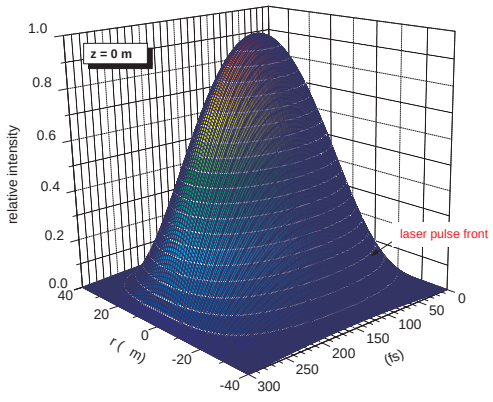

Figure 12: **Initial Laser Profile**

The particular test case: $I_0 = 1.5 \cdot 10^{13}$ W/cm^2, λ_0=800 nm, r_0=20 μm, T=300 fs, and E_0=3 mJ has the initial profile shown in Fig. 12. Such a pulse is advanced over space and time in 2D via the propagation model (§3.1.1).

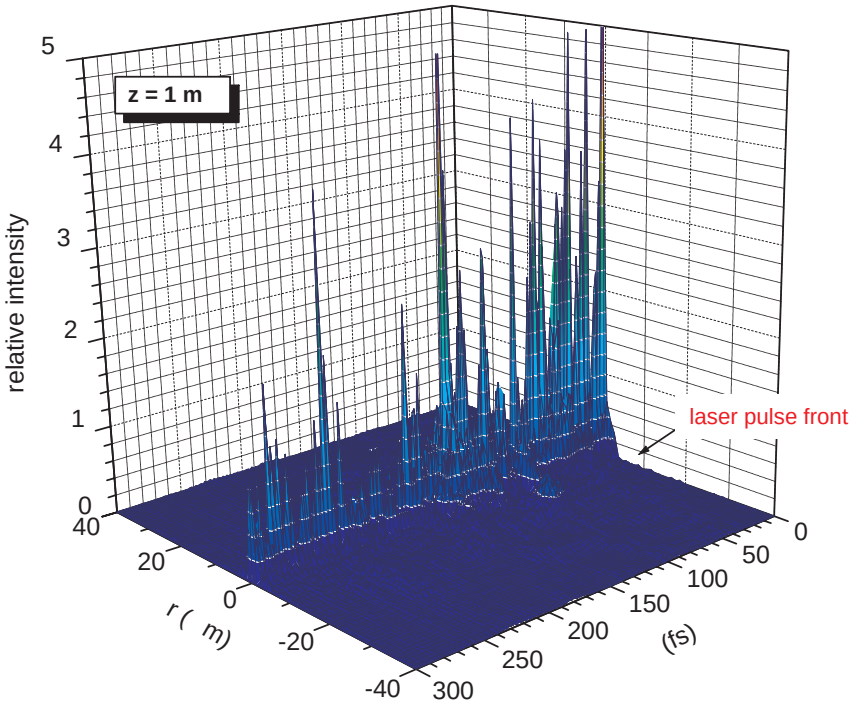

Figure 13: **Laser Profile at 1m**

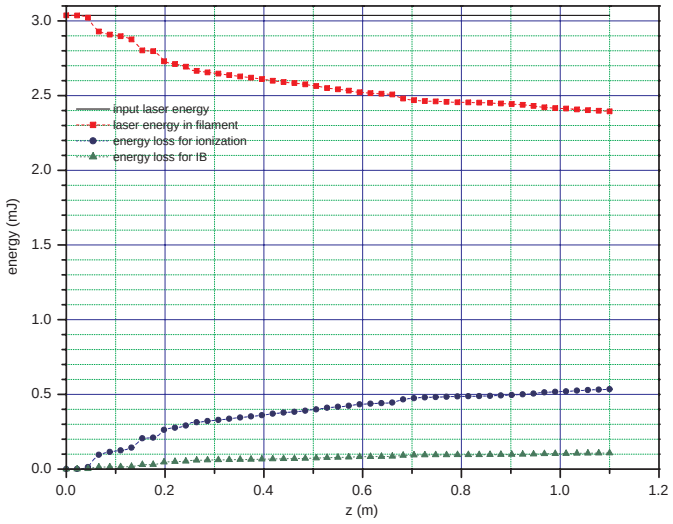

Figure 14: **Laser Attenuation with Distance**

The expected state of the laser filament after a meter of propagation is shown in Fig. 13, while the attenuation of the energy contained in the pulse is shown in Fig. 14. The observed damping decrement in this calculation is about 0.32 mJ/m in agreement with other work. Here the model works with only a single filament, a very idealized propagation mode. Yet, if this damping were to hold over 10m lengths, then a 50 mJ input pulse would still deliver 18 mJ in its envelope at 100 m. Such an intensity would be sufficient to support ionization throughout the channel.

4.2 Leader Propagation

To establish a good leader in a 100 m channel to a remote load, the high voltage pulse power subsystem will need to erect a bipolar 30-50 MV signal on each laser channel. With the typical resistances of the post leader medium at about 3.0 kΩ/cm the early discharge currents will be about 1 – 2 A and transfer only fraction of a Coulomb across the gap to set the channel.

4.3 Return Stroke Connection

As the return stroke discharges the voltage brought across by the leader, that connected channel breaks down to a quite lower impedance of perhaps 0.3 Ω/m or less. Now for the low voltage 100 m pulseline one needs only perhaps 300 – 500 kV DC to draw about 10 kA over the gap and help to "burn in" the channel even more. For these low frequency signals, the linear damping decrement δ should be modest but not severe. Frequencies of about 300 kHz should be about right for this component of the signals sent up the laser channel transmission line.

4.4 Pulse Launch, Control, and Delivery

For the higher power, more damaging, signals the frequency components should be in the domain of 30 MHz or higher. For this domain the damping decrement will be less than or about 0.05 and good coupling can obtain. The final design of the low voltage pulseline driver will therefore require some detailed attention to pulse shaping.

The damage to various loads can be expected to depend upon several mechanisms [9],[17],[24]. Simple Joule heating of a conducting skin may ignite secondary energy release within the load. Energy deposited in a plasma blanket evolved from a load surface may develop a significant impulse delivery to the load. Hence the experiment must examine energy delivery at a short distance first, even as small as a meter, and start to build a database of material responses.

5 New Features and Advantages

The principal innovations we advocate are (i) the use of a completed circuit of two laser channels rather than a single channel, (ii) the construction of both high voltage and low voltage pulse power subsystems for channel breakdown and final pulse delivery, (iii) a laser beam convolute to make connections to both the pulse power subsystems within a single element, and (iv) the maintenance of laser energies high enough for optical field ionization but lower than the fields required for avalanche ionization.

The dual channel arrangement serves to form a transmission line of low and controlled impedance, in contrast to any approach to sending power down a single laser channel. With only one conductor the system inductance is markedly larger and the frequency window for exciting low voltage pulses is thus curtailed to lower frequencies. The laser twin lead geometry admits essentially all RF frequencies as TEM pulses so that signals tailored to the target can be constructed if desired.

By convoluting separate high and low voltage pulse power systems into the laser beams we can solve two easier electrical engineering tasks instead on one difficult task. Each pulse system can be configured to operate on independent time bases and voltage domains with conventional technology.

Finally, by relying on optical field ionization by fast pulse lasers and feeding the laser energy into the channel in a measured way, we create a cold gas channel that will not tend to bloom out the laser beams. Moreover, by using the long lived species O_2^- as the charge reservoir, we can gain access to a physics domain capable of lowering the breakdown voltages needed to strike a low impedance lightening-like arc to the load.

References

[1] R. Ackermann, K. Stelmaszczyk, P. Rohwetter, G. Mejean, E. Salmon, J. Yu, J. Kasparian, G. Mechain, V. Bergmann, S. Schaper, B. Weise, T. Kumm, K. Rethmeier, W. Kalkner, L. Woste, and J. P. Wolf. Triggering and guiding of megavolt discharges by laser-induced filaments under rain conditions. *Applied Physics Letters*, 85(23):5781–5783, December 6 2004.

[2] N. L. Aleksandrov and E. M. Bazelyan. Streamer breakdown of long gas gaps. *Plasma Physics Reports*, 27(12):1057–1078, December 2001.

[3] E. Arevalo and A. Becker. Theoretical analysis of fluorescence signals in filamentation of femtosecond laser pulses in nitrogen molecular gas. *Physical Review A (Atomic, Molecular, and Optical Physics)*, 72(4):043807, October 2005.

[4] E. Arevalo and A. Becker. Variational analysis of self-focusing of intense ultrashort pulses in gases. *Physical Review E (Statistical, Nonlinear, and Soft Matter Physics)*, 72(2):026605, September 2005.

[5] L. Berge, S. Skupin, F. Lederer, G. Mejean, J. Yu, J. Kasparian, E. Salmon, and J. P. Wolf. Spatial break-up of femtosecond laser pulses in the atmosphere. *Physica Scripta*, T107:135–140, 2004.

[6] L. Berge, S. Skupin, F. Lederer, G. Mejean, J. Yu, J. Kasparian, E. Salmon, J. P. Wolf, M. Rodriguez, L. Woste, R. Bourayou, and R. Sauerbrey. Multiple filamentation of terawatt laser pulses in air. *Physical Review Letters*, 92(22):225002, June 4 2004.

[7] A. Braun, G. Korn, X. Liu, D. Du, J. Squier, and G. Mourou. Self-channeling of high-peak-power femtosecond laser-pulses in air. *Optics Letters*, 20(1):73–75, Jan 1 1995.

[8] A. Brodeur, C. Y. Chien, F. A. Ilkov, S. L. Chin, O. G. Kosareva, and V. P. Kandidov. Moving focus in the propagation of ultrashort laser pulses in air. *Optics Letters*, 22(5):304–306, Mar 1 1997.

[9] Changrui Cheng and Xianfan Xu. Mechanisms of decomposition of metal during femtosecond laser ablation. *Physical Review B (Condensed Matter and Materials Physics)*, 72(16):165415, October 15 2005.

[10] D. Comtois, H. Pepin, F. Vidal, F. A. M. Rizk, Ching-Yuan Chien, T. W. Johnston, J. C Kieffer, B. La Fontaine, F. Martin, C. Potvin, P. Couture, H. P. Mercure, A. Bondiou-Clergerie, P. Lalande, and I. Gallimberti. Triggering and guiding of an upward positive leader from a ground rod with an ultrashort laser pulse. i. experimental results. *Plasma Science, IEEE Transactions on*, 31(3):377–386, 2003.

[11] D. Comtois, H. Pepin, F. Vidal, F. A. M. Rizk, Ching-Yuan Chien, T. W. Johnston, J. C Kieffer, B. La Fontaine, F. Martin, C. Potvin, P. Couture, H. P. Mercure, A. Bondiou-Clergerie, P. Lalande, and I. Gallimberti. Triggering and guiding of an upward positive leader from a ground rod with an ultrashort laser pulse. ii. modeling. *Plasma Science, IEEE Transactions on*, 31(3):387–395, 2003.

[12] G. V. Cooray. *The Lightning Flash*, volume 34. IEE, U.K., 2003. pp. 160-170.

[13] A. Couairon, G. Mechain, S. Tzortzakis, M. Franco, B. Lamouroux, B. Prade, and A. Mysyrowicz. Propagation of twin laser pulses in air and concatenation of plasma strings produced by femtosecond infrared filaments. *Optics Communications*, 225(1):177, 2003.

[14] Bruno La Fontaine, Daniel Comtois, Ching-Yuan Chien, Alain Desparois, Frederic Genin, Genevieve Jarry, Tudor Johnston, Jean-Claude Kieffer, Francois Martin, Raafat Mawassi, Henri Pepin, Farouk A. M. Rizk, Francois Vidal, Carl Potvin, Pierre Couture, and Hubert P. Mercure. Guiding large-scale spark discharges with ultrashort pulse laser filaments. *Journal of Applied Physics*, 88(2):610–615, July 15 2000.

[15] M. V. Frolov, A. V. Flegel, N. L. Manakov, and Anthony F. Starace. Rescattering effects in the multiphoton regime. *Journal of Physics B: Atomic, Molecular and Optical Physics*, (23):L375–L382, 2005.

[16] E. Frumker, Eran Tal, Y. Silberberg, and D. Majer. Femtosecond pulse-shape modulation at nanosecond rates. *Optics Letters*, 30(20):2796–2798, October 15 2005.

[17] Allan Gibson. Laser pointing technology. volume 4034, pages 165–174. SPIE, July 21 2000.

[18] D. F. Gordon, A. Ting, R. F. Hubbard, E. Briscoe, C. Manka, S. P. Slinker, A. P. Baronavski, H. D. Ladouceur, P. W. Grounds, and P. G. Girardi. Streamerless guided electric discharges triggered by femtosecond laser filaments. *Physics of Plasmas*, 10(11):4530–4538, November 2003.

[19] Nasrullah Khan, Norman Mariun, Ishak Aris, and J. Yeak. Laser-triggered lightning discharge. *New Journal of Physics*, pages 61–61, 2002.

[20] David W. Koopman and T. D. Wilkerson. Channeling of an ionizing electrical streamer by a laser beam. *Journal of Applied Physics*, 42(5):1883–1886, April 1971.

[21] Jiansheng Liu, Zuoliang Duan, Zhinan Zeng, Xinhua Xie, Yunpei Deng, Ruxin Li, Zhizhan Xu, and See Leang Chin. Time-resolved investigation of low-density plasma channels produced by a kilohertz femtosecond laser in air. *Physical Review E (Statistical, Nonlinear, and Soft Matter Physics)*, 72(2):026412, August 2005.

[22] W. Liu and S. L. Chin. Direct measurement of the critical power of femtosecond ti:sapphire laser pulse in air. *Optics Express*, 13(15):5750–5755, July 25 2005.

[23] Q. Luo, J. Yu, S. A. Hosseini, W. W. Liu, B. Ferland, G. Roy, and S. L. Chin. Long-range detection and length estimation of light filaments using extra-attenuation of terawatt femtosecond laser pulses propagating in air. *Applied Optics*, 44(3):391–397, Jan 20 2005.

[24] Alan J. MacGovern, David A. Nahrstedt, and Michael M. Johnson. Atmospheric propagation for tactical directed-energy applications. volume 4034, pages 128–139. SPIE, July 21 2000.

[25] G. Mechain, A. Couairon, M. Franco, B. Prade, and A. Mysyrowicz. Organizing multiple femtosecond filaments in air. *Physical Review Letters*, 93(3):035003, July 16 2004.

[26] G. Mechain, C. D'Amico, Y. B Andre, S. Tzortzakis, M. Franco, B. Prade, A. Mysyrowicz, A. Couairon, E. Salmon, and R. Sauerbrey. Range of plasma filaments created in air by a multi-terawatt femtosecond laser. *Optics Communications*, 247(1):171, 2005.

[27] Zoltan Mics, Filip Kadlec, Petr Kuzel, Pavel Jungwirth, Stephen E. Bradforth, and V. Ara Apkarian. Nonresonant ionization of oxygen molecules by femtosecond pulses: Plasma dynamics studied by time-resolved terahertz spectroscopy. *The Journal of Chemical Physics*, 123(10):104310, 8 September 2005.

[28] M. Mlejnek, E. M. Wright, and J. V. Moloney. Dynamic spatial replenishment of femtosecond pulses propagating in air. *Optics Letters*, 23(5):382–384, Mar 1 1998.

[29] P. Paris, M. Aints, M. Laan, and T. Plank. Laser-induced current in air gap at atmospheric pressure. *Journal of Physics D: Applied Physics*, (21):3900–3906, 2005.

[30] Y. P. Raizer. *Gas Discharge Physics*. Springer-Verlag, New York, 1991. pp.324 ff.

[31] T. V. Rao. Capacity of the circular plate condenser: analytical solutions for large gaps between the plates. *Journal of Physics A: Mathematical and General*, (46):10037–10056, 2005.

[32] M. Rodriguez, R. Sauerbrey, H. Wille, L. Woste, T. Fujii, Y. B. Andre, A. Mysyrowicz, L. Klingbeil, K. Rethmeier, W. Kalkner, J. Kasparian, E. Salmon, J. Yu, and J. P. Wolf. Triggering and guiding megavolt discharges by use of laser-induced ionized filaments. *Optics Letters*, 27(9):772–774, May 1 2002.

[33] Miguel Rodriguez, Riad Bourayou, Guillaume Mejean, Jerome Kasparian, Jin Yu, Estelle Salmon, Alexander Scholz, Bringfried Stecklum, Jochen Eisloffel, Uwe Laux, Artie P. Hatzes, Roland Sauerbrey, Ludger Woste, and Jean-Pierre Wolf. Kilometer-range nonlinear propagation of femtosecond laser pulses. *Physical Review E (Statistical, Nonlinear, and Soft Matter Physics)*, 69(3):036607, March 2004.

[34] K. A. Saum and D. W. Koopman. Discharges guided by laser-induced rarefaction channels. *Physics of Fluids*, 15(11):2077, 1972.

[35] J. Schwarz, P. Rambo, and J. C. ER . Diels. Measurements of multiphoton ionization coefficients with ultrashort ultraviolet laser pulses. *Applied Physics B: Lasers and Optics*, 72(3):343–347, February 2001.

[36] Jens Schwarz and Jean-Claude Diels. Analytical solution for uv filaments. *Physical Review A (Atomic, Molecular, and Optical Physics)*, 65(1):013806, January 2002.

[37] Yoshinori Shimada, Shigeaki Uchida, Hirohiko Yasuda, Shinji Motokoshi, Chiyoe Yamanaka, Zen ichiro Kawasaki, Tatsuhiko Yamanaka, Yuji Ishikubo, and Mikio Adachi. Laser-triggered lightning. volume 3423, pages 258–261. SPIE, July 14 1998.

[38] F. Vidal, D. Comtois, Ching-Yuan Chien, A. Desparois, B. La Fontaine, T. W. Johnston, J. C Kieffer, H. P. Mercure, H. Pepin, and F. A. Rizk. Modeling the triggering of streamers in air by ultrashort laser pulses. *Plasma Science, IEEE Transactions on*, 28(2):418–433, 2000.

[39] P. A. Vitello, B. M. Penetrante, and J. N. Bardsley. Simulation of negative-streamer dynamics in nitrogen. *Physical Review E*, 49(6):5574–5598, Jun 1994.

[40] Tatsuhiko Yamanaka, Shigeaki Uchida, Yoshinori Shimada, Hirohiko Yasuda, Shinji Motokoshi, Kouji Tsubakimoto, Zen ichiro Kawasaki, Yuji Ishikubo, Mikio Adachi, and Chiyoe Yamanaka. First observation of laser-triggered lightning. volume 3343, pages 281–288. SPIE, September 14 1998.